Journal of Statistical Physics, Vol. 107, Nos. 1/2, April 2002 (© 2002)

Numerical Stability Analysis of FDLBM

Takeshi Seta[1] **and Ryoichi Takahashi**[2]

Received February 14, 2001

We analyze the numerical stability of Finite Difference Lattice Boltzmann Method (FDLBM) by means of von Neumann stability analysis. The stability boundary of the FDLBM depends on the BGK relaxation time, the CFL number, the mean flow velocity, and the wavenumber. As the BGK relaxation time is increased at constant CFL number, the stability of the central difference LB scheme may not be ensured. The limits of maximum stable velocity are obtained around 0.39, 0.43, and 0.43 for the central difference, for the explicit upwind difference, and for the semi-implicit upwind difference schemes, respectively. We derive artificial viscosities for every difference scheme and investigate their influence on numerical stability. The requirements for artificial viscosity is consistent with the conditions derived from von Neumann stability analysis. This analysis elucidates that the upwind difference schemes are suitable for simulation of high Reynolds number flows.

KEY WORDS: Numerical stability; finite difference lattice Boltzmann method; artificial viscosity; von Neumann stability analysis.

1. INTRODUCTION

In recent years, the lattice gas automata (LGA)[1] or the lattice Boltzmann method (LBM)[2, 3] has received considerable attention as an alternative numerical scheme for simulating complex phenomena. The LBM resolved the problems of the lattice gas automata: it removed statistical noise and eliminated the spurious invariants in the Navier–Stokes equations. The LB method could, however, be numerically unstable for high Reynolds number flows or for thermal problems.

[1] Shizuoka Sangyo University, Department of Business Administration, 1572-1 Ohara, Iwata-city, Shizuoka 438-0043, Japan; e-mail: c1seta@ssu.ac.jp

[2] Shizuoka Sangyo University, Department of Communications and Informatics, Fujieda, Japan.

0022-4715/02/0400-0557/0 © 2002 Plenum Publishing Corporation

In the LBM, the particle velocity distribution function approaches toward Maxwell–Boltzmann distribution function equivalent to the maximum entropy state. In traditional kinetic theory, Boltzmann's H-theorem ensures increases of entropy[4] which is indicated by second law of thermodynamics. If any initial states of the LBM evolve toward an equilibrium state, the stability can be guaranteed.[5] The LBM, however, cannot usually find an equilibrium distribution function that can simultaneously guarantee the H-theorem and recover correct form of macroscopic conservation equations.[4] For reasons mentioned above, the LBM needs suitable condition to stably simulate fluid dynamics.

Sterling *et al.* analyzed the numerical stability of the LBMs for the incompressible Navier–Stokes equations and reported results as follows:[4] (1) the BGK relaxation time τ must be greater than $\frac{1}{2}$, (2) The limits of the maximum stable mean flow velocity are around 0.39, 0.42, and 0.47 for a 7-velocity hexagonal, a 9-velocity square, and a 15-velocity cubic lattices, respectively, (3) as τ is increased from $\frac{1}{2}$, the maximum stable velocity increases monotonically until some fixed velocity is reached which does not change for larger τ.

The LBMs were originated from the lattice gas automata (LGA), their Boolean counterparts. The LBM can also be viewed as a special discretization of Boltzmann equation for the discrete-velocity distribution function. The discrete-velocity gas that is composed of identical particles with velocities restricted to a finite set has been used to solve the Boltzmann equation by several authors. Broadwell applied two simple discrete-velocity models to low Mach number Couette and Rayleigh flows.[6, 7] Gatignol investigated boundary conditions and gas surface interaction with four coplanar velocities.[8, 9] Nadiga *et al.* extensively worked on this approach, and presented a simulation scheme for discrete-velocity gases based on local thermodynamic equilibrium.[10] Inamuro *et al.* used discrete-velocity models, in which molecules have many discrete velocities, for studying shock-wave structures and heat transfer.[11] Though all these models utilized the discrete velocity distribution, space and time were continuous. The LGA involves space and time discretized on a square lattice in addition to a discretization of the velocity space.[12] Frisch *et al.* pointed out the importance of the symmetry of the lattice to obtain correct form of the Navier–Stokes equation.[1]

Cao *et al.* proposed the FDLBM that improved the numerical stability of the LBM.[13] Lattice symmetry and Lagrangian nature of the scheme, which are used in the LBM, are directly associated with the property of particle dynamics. On the other hand, the physical symmetry is necessary for obtaining the correct form of macroscopic momentum conservation equations from the kinetic equations of the LBM. As shown in Fig. 1, the

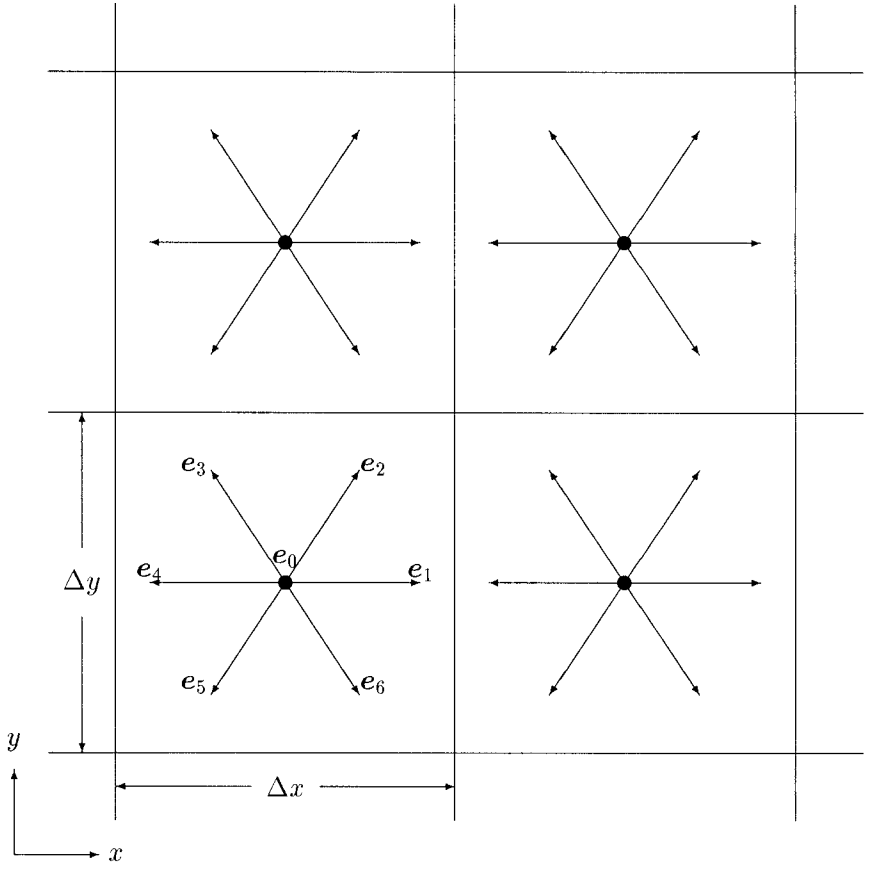

Fig. 1. Schematic of a hexagonal lattice in FDLBM.

FDLBM separates the physical symmetry from the lattice symmetry, so that the grid size is handled independently of the discrete particle velocity. Regardless of the magnitude of triangle lattice (i.e., the magnitude of discrete particle velocity), we can set the grid sizes, Δx and Δy (see Fig. 1). The FDLBM that utilizes this separation is regarded as the above-mentioned discrete-velocity method, although the formulation of the equilibrium distribution function is different from the discrete-velocity models. As is generally known, in both these methods, the physically relevant discretization is that of the velocity space: the discretization of space and time is a numerical necessity and importantly is not tied to the discretization of the velocity space.

The numerical stability of the FDLBM has not been sufficiently evaluated. The numerical stability of the FDLBM is affected by changing finite difference approximation which discretizes the evolution equation. We analyze the stability of the FDLBM discretized by representative finite difference approximations, that is, the central difference, the explicit upwind difference, and the semi-implicit upwind difference approximations. The stability boundaries are shown as function of the CFL number, the BGK relaxation time, the mean flow velocity, and the wavenumber.

2. FDLBM

In the FDLBM, instead of standard kinetic equation in the LBM, the following approximated Boltzmann equation for the discrete velocity distribution function f_i:

$$\frac{\partial f_i(\mathbf{x}, t)}{\partial t} + \mathbf{e}_i \cdot \nabla f_i(\mathbf{x}, t) = \Omega_i(\mathbf{x}, t), \qquad (i = 1, 2, \ldots, N) \tag{1}$$

is calculated with the finite difference method, where $\mathbf{e}_i$ is the unit velocity vector along the ith direction in space, N is the number of directions of velocity, and Ω_i is the collision operator. t is time variable, and $\mathbf{x}$ is space variable on the lattice. In general, the BGK collision operator,

$$\Omega_i(\mathbf{x}, t) = -\frac{f_i(\mathbf{x}, t) - f_i^{(0)}(\mathbf{x}, t)}{\varepsilon\tau} \tag{2}$$

is applied to Eq. (1), where $f_i^{(0)}$ is the local equilibrium distribution function, τ is the relaxation time, and ε is a small parameter, proportional to the Knudsen number. We use the two-dimensional 7-velocity hexagonal lattice with one rest particle: $\mathbf{e}_0 = (0, 0)$, and moving particles with nonzero velocity vectors: $\mathbf{e}_i = (\cos((\pi(i-1))/3), \sin((\pi(i-1))/3))$, $(i = 1, \ldots, 6)$.

The equilibrium distribution function $f_i^{(0)}$ is given by a truncated power series in the local velocity $\mathbf{u}$ assuming $\mathbf{u} \ll 1$:

$$f_0^{(0)} = \rho(\theta - u^2) \tag{3}$$

$$f_i^{(0)} = \rho\left(\frac{(1-\theta)}{6} + \frac{1}{3}\mathbf{e}_i \cdot \mathbf{u} + \frac{2}{3}(\mathbf{e}_i \cdot \mathbf{u})^2 - \frac{1}{6}u^2\right), \qquad (i = 1, \ldots, 6) \tag{4}$$

where θ is a constant that determines the distribution of mass between the moving and nonmoving populations.[14] Hydrodynamical quantities,

including the density ρ and momentum ρu_α, are defined through the moments of the distribution function f_i as

$$\sum_i f_i = \rho, \qquad \sum_i f_i (e_i)_\alpha = \rho u_\alpha \tag{5}$$

Applying the standard Chapman–Enskog procedure[15] to Eq. (1), one obtains the equation of continuity,

$$\frac{\partial \rho}{\partial t} + \frac{\partial \rho u_\alpha}{\partial x_\alpha} = 0 \tag{6}$$

and the momentum equations,

$$\frac{\partial \rho u_\alpha}{\partial t} + \frac{\partial \rho u_\alpha u_\beta}{\partial x_\beta} = -\frac{\partial P}{\partial x_\alpha} + \frac{\partial}{\partial x_\alpha}\left[\frac{\lambda}{\rho}\frac{\partial \rho u_\beta}{\partial x_\beta}\right] + \frac{\partial}{\partial x_\beta}\left[\mu\left[\frac{\partial u_\beta}{\partial x_\alpha} + \frac{\partial u_\alpha}{\partial x_\beta}\right]\right] \tag{7}$$

where P is the pressure, μ and λ are the shear viscosity and the second viscosity, respectively. The Greek subscripts α and β denote the space directions in Cartesian coordinates. The shear viscosity μ, the second viscosity λ, and the sound speed C_s are given by $\mu = \rho\varepsilon\tau/4$, $\lambda = \rho\varepsilon\tau(2\theta - 1)/4$, and $C_s = \sqrt{\frac{(1-\theta)}{2}}$, respectively.

3. VON NEUMANN STABILITY ANALYSIS

We analyze the numerical stability of the FDLBM by means of von Neumann stability analysis.[16] In the von Neumann analysis, the solution of finite difference equation is written as the familiar Fourier series, and the numerical stability is evaluated by the magnitude of eigenvalues of an amplification matrix. The small perturbation Δf_i is defined as

$$f_i(\mathbf{x}, t) = \Delta f_i(\mathbf{x}, t) + \overline{f_i^{(0)}} \tag{8}$$

where $\overline{f_i^{(0)}}$ is distribution function at constant density and flow velocity.

Taking Taylor series expansion of Eq. (1) around the equilibrium value for certain density and flow velocity, we obtain the following equation,

$$\frac{\partial}{\partial t}\Delta f_i(\mathbf{x}, t) + \mathbf{e}_i \cdot \nabla(\Delta f_i(\mathbf{x}, t)) = \left(\frac{\partial \Omega_i}{\partial \rho}\frac{\partial \rho}{\partial f_j} + \frac{\partial \Omega_i}{\partial \rho u_\alpha}\frac{\partial \rho u_\alpha}{\partial f_j}\right)\Delta f_j(\mathbf{x}, t) \tag{9}$$

The solution may be written as series of complex exponentials,

$$\Delta f_i(\mathbf{x}, t) = F_i^t \exp(\mathbf{i}k\mathbf{x}) \tag{10}$$

where F_i^t is an amplitude at grid point i and time t, $\mathbf{i}$ is an imaginary unit, and k is a wavenumber.

Inserting Eq. (10) into Eq. (9) yields amplification matrix $G_{i,j}$ as,

$$F_i^{t+\Delta t} = G_{i,j} F_j^t \tag{11}$$

The amplification matrix $G_{i,j}$ is made use of assessing amplification rate of F_i^t per time step Δt. If the maximum of the eigenvalues of the amplification matrix satisfies the following condition:

$$\max |\omega| \leqslant 1 \tag{12}$$

for all wavenumbers, the finite difference scheme is determined to be numerically stable. ω is the eigenvalue of the amplification matrix. Equation (12) is called the von Neumann condition for stability.

To obtain the second order accuracy, likewise with the conventional LBM,[17] the FDLBM needs to apply the second order central difference approximation to Eq. (1). For steep density gradients problem, e.g., shock waves or interfaces in two-phase flow, the first order upwind difference scheme leads to stable simulation without any numerical oscillations. From the above-mentioned reason, we analyze the numerical stability of the three kinds of FDLB schemes, that is, the explicit central, the explicit upwind, and semi-implicit upwind difference schemes.

If the explicit central difference scheme is applied to Eq. (1) as

$$\frac{f_i(\mathbf{x}, t+\Delta t) - f_i(\mathbf{x}, t)}{\Delta t} + (\mathbf{e}_i)_\alpha \frac{f_i(x_\alpha + \Delta x_\alpha, t) - f_i(x_\alpha - \Delta x_\alpha, t)}{2\Delta x_\alpha} = -\frac{f_i(\mathbf{x}, t) - f_i^{(0)}(\mathbf{x}, t)}{\varepsilon\tau} \tag{13}$$

the amplification matrix becomes

$$G_{i,j} = \left(1 - \frac{c_\alpha(\exp(\mathbf{i}k\,\Delta x_\alpha) - \exp(-\mathbf{i}k\,\Delta x_\alpha))}{2} - \frac{\Delta t}{\varepsilon\tau}\right)\delta_{ij} + \frac{\Delta t}{\varepsilon\tau}\left(\frac{\partial f_i^{(0)}}{\partial \rho}\frac{\partial \rho}{\partial f_j} + \frac{\partial f_i^{(0)}}{\partial \rho u_\alpha}\frac{\partial \rho u_\alpha}{\partial f_j}\right) \tag{14}$$

where δ_{ij} is the Kronecker delta function. Similarly, if the explicit upwind difference scheme, which utilizes the forward time difference and the upwind space difference, is applied to Eq. (1) as

$(e_i)_\alpha \geqslant 0$:

$$\frac{f_i(\mathbf{x}, t+\Delta t)-f_i(\mathbf{x}, t)}{\Delta t}+(e_i)_\alpha \frac{f_i(x_\alpha, t)-f_i(x_\alpha-\Delta x_\alpha, t)}{\Delta x_\alpha} = -\frac{f_i(\mathbf{x}, t)-f_i^{(0)}(\mathbf{x}, t)}{\varepsilon\tau} \tag{15}$$

$(e_i)_\alpha < 0$:

$$\frac{f_i(\mathbf{x}, t+\Delta t)-f_i(\mathbf{x}, t)}{\Delta t}+(e_i)_\alpha \frac{f_i(x_\alpha+\Delta x_\alpha, t)-f_i(x_\alpha, t)}{\Delta x_\alpha} = -\frac{f_i(\mathbf{x}, t)-f_i^{(0)}(\mathbf{x}, t)}{\varepsilon\tau} \tag{16}$$

the amplification matrix is

$(e_i)_\alpha \geqslant 0$:

$$G_{i,j}=\left(1-c_\alpha(1-\exp(-\mathbf{i}k\,\Delta x_\alpha))-\frac{\Delta t}{\varepsilon\tau}\right)\delta_{ij}+\frac{\Delta t}{\varepsilon\tau}\left(\frac{\partial f_i^{(0)}}{\partial\rho}\frac{\partial\rho}{\partial f_j}+\frac{\partial f_i^{(0)}}{\partial\rho u_\alpha}\frac{\partial\rho u_\alpha}{\partial f_j}\right) \tag{17}$$

$(e_i)_\alpha < 0$:

$$G_{i,j}=\left(1-c_\alpha(\exp(\mathbf{i}k\,\Delta x_\alpha)-1)-\frac{\Delta t}{\varepsilon\tau}\right)\delta_{ij}+\frac{\Delta t}{\varepsilon\tau}\left(\frac{\partial f_i^{(0)}}{\partial\rho}\frac{\partial\rho}{\partial f_j}+\frac{\partial f_i^{(0)}}{\partial\rho u_\alpha}\frac{\partial\rho u_\alpha}{\partial f_j}\right) \tag{18}$$

If the semi-implicit upwind difference scheme is applied to Eq. (1) as

$(e_i)_\alpha \geqslant 0$:

$$\frac{f_i(\mathbf{x}, t+\Delta t)-f_i(\mathbf{x}, t)}{\Delta t}+(e_i)_\alpha \frac{f_i(x_\alpha, t+\Delta t)-f_i(x_\alpha-\Delta x_\alpha, t+\Delta t)}{\Delta x_\alpha} = -\frac{f_i(\mathbf{x}, t)-f_i^{(0)}(\mathbf{x}, t)}{\varepsilon\tau} \tag{19}$$

$(e_i)_\alpha < 0$:

$$\frac{f_i(\mathbf{x}, t+\Delta t)-f_i(\mathbf{x}, t)}{\Delta t}+(e_i)_\alpha \frac{f_i(x_\alpha+\Delta x_\alpha, t+\Delta t)-f_i(x_\alpha, t+\Delta t)}{\Delta x_\alpha} = -\frac{f_i(\mathbf{x}, t)-f_i^{(0)}(\mathbf{x}, t)}{\varepsilon\tau} \tag{20}$$

the amplification matrix becomes

$(e_i)_\alpha \geqslant 0$:

$$G_{i,j} = \frac{\left(1-\frac{\Delta t}{\varepsilon\tau}\right)\delta_{ij} + \frac{\Delta t}{\varepsilon\tau}\left(\frac{\partial f_i^{(0)}}{\partial \rho}\frac{\partial \rho}{\partial f_j} + \frac{\partial f_i^{(0)}}{\partial \rho u_\alpha}\frac{\partial \rho u_\alpha}{\partial f_j}\right)}{1 + c_\alpha(1-\exp(-\mathbf{i}k\,\Delta x_\alpha))} \tag{21}$$

$(e_i)_\alpha < 0$:

$$G_{i,j} = \frac{\left(1-\frac{\Delta t}{\varepsilon\tau}\right)\delta_{ij} + \frac{\Delta t}{\varepsilon\tau}\left(\frac{\partial f_i^{(0)}}{\partial \rho}\frac{\partial \rho}{\partial f_j} + \frac{\partial f_i^{(0)}}{\partial \rho u_\alpha}\frac{\partial \rho u_\alpha}{\partial f_j}\right)}{1 + c_\alpha(\exp(\mathbf{i}k\,\Delta x_\alpha)-1)} \tag{22}$$

4. STABILITY ANALYSIS FOR FINITE DIFFERENCE LATTICE BOLTZMANN SCHEME

The first analysis shows stability boundary of the FDLBM, as function of the CFL number $|\mathbf{e}_i|\,\Delta t/\Delta x$ and the relaxation time of the FDLBM $\varepsilon\tau$, for three kinds of the finite difference schemes. The mean flow velocity and wavenumber are both vectors. Although there is not sufficient proof, from the result for the case studied, the most unstable condition occurred when the angle between the vectors were equal to zero.[4] The mean flow velocity and wavenumber are assumed to be parallel to the horizontal axis. When the relaxation time $\tau = 1$, the slip velocities generated by various schemes for the nonslip boundaries become zero.[18] When τ is large, the mean-free path becomes large and the Chapman–Enskog procedure breaks down.[19, 20] The FDLBM relaxation time $\varepsilon\tau$ and the CFL number are from 0.00 to 2.00 in steps of 0.02 for every following analysis. In the LBM, when using a unit lattice spacing, the highest resolvable wavenumber is equal to π.[4] To compare with the LBM,[4] we analyze the numerical stability of the FDLBM at the wavenumber less than π. The maximum stable mean flow velocity of the conventional 7-velocity hexagonal LBM is about 0.39.[4] This value is obtained by selecting $\theta = 0.7$. To compare with the LBM, the subsequent simulation uses the distribution parameter, $\theta = 0.7$. The eigenvalues of $G_{i,j}$ are determined using *Matlab* Version 5.3.1.

Figure 2 shows the stability boundaries for various wavenumbers at zero mean flow velocity. The stability boundaries depend on the relaxation time, and the CFL number. The results for the explicit central difference, for the explicit upwind difference, and for the semi-implicit upwind difference schemes, are shown in (a), (b), and (c), respectively. Figure 2a shows that, as the BGK relaxation time is increased at constant CFL number, the central difference LB scheme could be unstable. This is characteristic

opposite to that of the conventional LBM. In the LBM, increment of the relaxation time makes the LBM more stable. In our simulation of Poiseuille flow, when the relaxation time was larger than unity, the numerical solution calculated by the central difference LB scheme diverged. As is evident from Fig. 2a, when using the central difference scheme, the FDLBM researchers need to take note of setting the parameter $\varepsilon\tau \simeq 1$ or using small CFL number for stable numerical simulation. Figure 2 shows that the FDLBM eliminates the condition for the LBM: $\tau > 0.5$ independently of ε. This fact allows the FDLBM to simulate the high Reynolds number flow, if CFL number is appropriately given. Figure 2a indicates that the central difference scheme is the most unstable when the wave number equals to 0.50π. Figure 2b tells us that as the wavenumber becomes higher, the stability region for explicit upwind difference becomes smaller. Figure 2c shows that the increment of wavenumber makes the semi-implicit upwind difference scheme less stable. This is an opposite result to Fig. 2b. It is difficult to obtain the single wavenumber that always makes all the FDLB schemes the least stable.

Figure 3 shows the stability regions of the three kinds of finite difference schemes applied the mean flow velocities. In this simulation, we analyze the numerical stability for all wavenumbers from $\pi/20$ to $19\pi/20$ in steps of $\pi/20$. As the mean flow velocity is increased, the sizes of the stability regions for every scheme reduce. We determine the limits of maximum stable velocities for every scheme within the limits of CFL number from 0.00 to 2.00, and relaxation time from 0.00 to 2.00. The limits are obtained around 0.39, 0.43, and 0.43 for the central difference, for the explicit upwind difference, and for the semi-implicit upwind difference schemes, respectively. As Fig. 3a indicates, as the relaxation time is increased, the central difference LB scheme becomes more stable for large flow velocity when the CFL number is sufficiently small. It seems reasonable to conclude that the central difference LB scheme possesses the numerical stability limit against the Reynolds number, similarly to the conventional LBM. On the other hand, as shown in Fig. 3b, c, as the relaxation time is decreased, the upwind difference schemes become more stable for large flow velocity. This is very useful property to simulate high Reynolds number flow. Furthermore, comparison between Fig. 3b and c makes it clear that the semi-implicit upwind difference LB scheme is more stable than the explicit upwind difference LB scheme for high CFL number.

5. ARTIFICIAL VISCOSITY

In this section, we verify the effect of artificial viscosities for every difference scheme on numerical stability. To determine the artificial viscosity

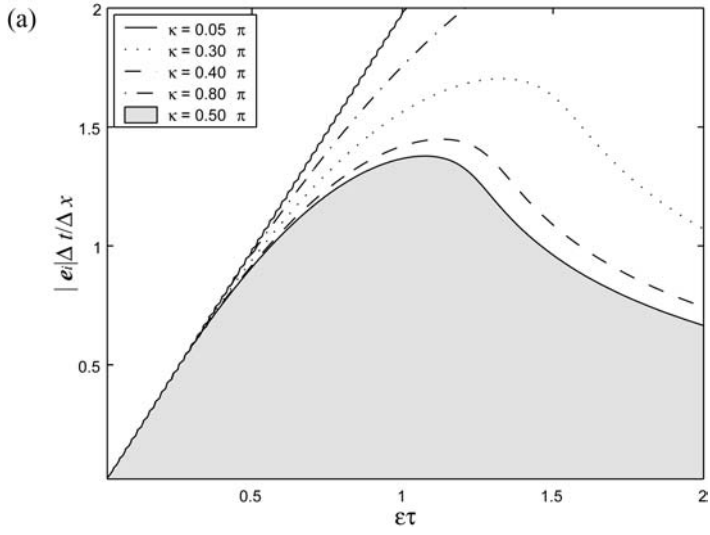

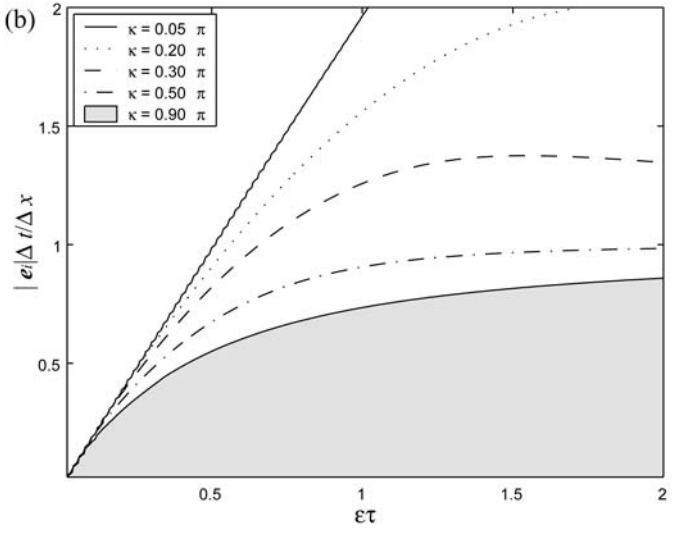

Fig. 2. Stability boundaries as function of Courant number and relaxation time. The wavenumber is less than π: (a) the explicit central difference; (b) the explicit upwind difference; (c) the semi-implicit upwind difference.

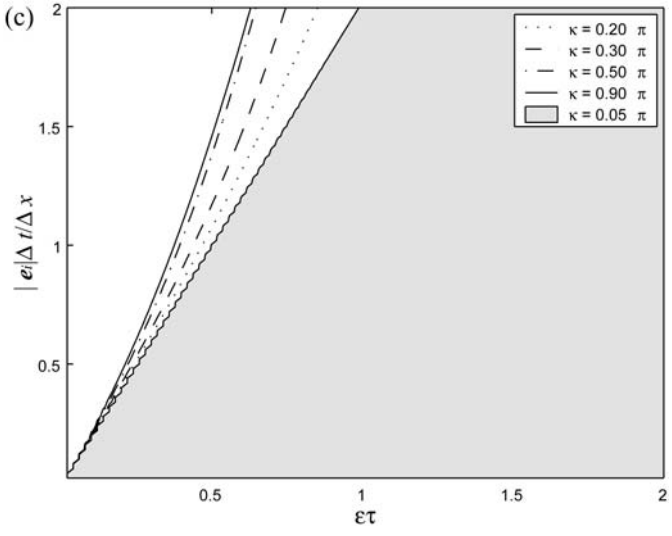

Fig. 2. (Continued).

for the explicit upwind difference scheme, taking Taylor series expansion of $f_i(\mathbf{x}, t+\Delta t)$ around $f_i(\mathbf{x}, t)$ gives

$$f_i(\mathbf{x}, t+\Delta t) = f_i(\mathbf{x}, t) + \Delta t \frac{\partial f_i(\mathbf{x}, t)}{\partial t} + \frac{\Delta t^2}{2} \frac{\partial^2 f_i(\mathbf{x}, t)}{\partial t^2} + \frac{\Delta t^3}{6} \frac{\partial^3 f_i(\mathbf{x}, t)}{\partial t^3} + \cdots \tag{23}$$

Similarly, taking Taylor series expansion of $f_i(\mathbf{x}-\Delta\mathbf{x}, t)$, one gets

$$f_i(\mathbf{x}-\Delta\mathbf{x}, t) = f_i(\mathbf{x}, t) - \Delta\mathbf{x} \frac{\partial f_i(\mathbf{x}, t)}{\partial \mathbf{x}} + \frac{\Delta\mathbf{x}^2}{2} \frac{\partial^2 f_i(\mathbf{x}, t)}{\partial \mathbf{x}^2} - \frac{\Delta\mathbf{x}^3}{6} \frac{\partial^3 f_i(\mathbf{x}, t)}{\partial \mathbf{x}^3} + \cdots \tag{24}$$

Substituting Eqs. (23) and (24) into the LHS in Eq. (15) gives

$$\begin{aligned}
&\frac{f_i(\mathbf{x}, t+\Delta t) - f_i(\mathbf{x}, t)}{\Delta t} + (\mathbf{e}_i)_\alpha \frac{f_i(x_\alpha, t) - f_i(x_\alpha - \Delta x_\alpha, t)}{\Delta x_\alpha} \\
&= \frac{\partial f_i(\mathbf{x}, t)}{\partial t} + \frac{\Delta t}{2} \frac{\partial^2 f_i(\mathbf{x}, t)}{\partial t^2} + (\mathbf{e}_i)_\alpha \left(\frac{\partial f_i(x_\alpha, t)}{\partial x_\alpha} - \frac{\Delta x_\alpha}{2} \frac{\partial^2 f_i(x_\alpha, t)}{\partial x_\alpha^2} \right) \\
&= \frac{\partial f_i(\mathbf{x}, t)}{\partial t} + \frac{\Delta t (\mathbf{e}_i)_\alpha^2}{2} \frac{\partial^2 f_i(x_\alpha, t)}{\partial x_\alpha^2} + (\mathbf{e}_i)_\alpha \left(\frac{\partial f_i(x_\alpha, t)}{\partial x_\alpha} - \frac{\Delta x_\alpha}{2} \frac{\partial^2 f_i(x_\alpha, t)}{\partial x_\alpha^2} \right) \\
&= \frac{\partial f_i(\mathbf{x}, t)}{\partial t} + (\mathbf{e}_i)_\alpha \frac{\partial f_i(x_\alpha, t)}{\partial x_\alpha} - \frac{(\mathbf{e}_i)_\alpha \Delta x_\alpha (1 - c_\alpha)}{2} \frac{\partial^2 f_i(x_\alpha, t)}{\partial x_\alpha^2}
\end{aligned} \tag{25}$$

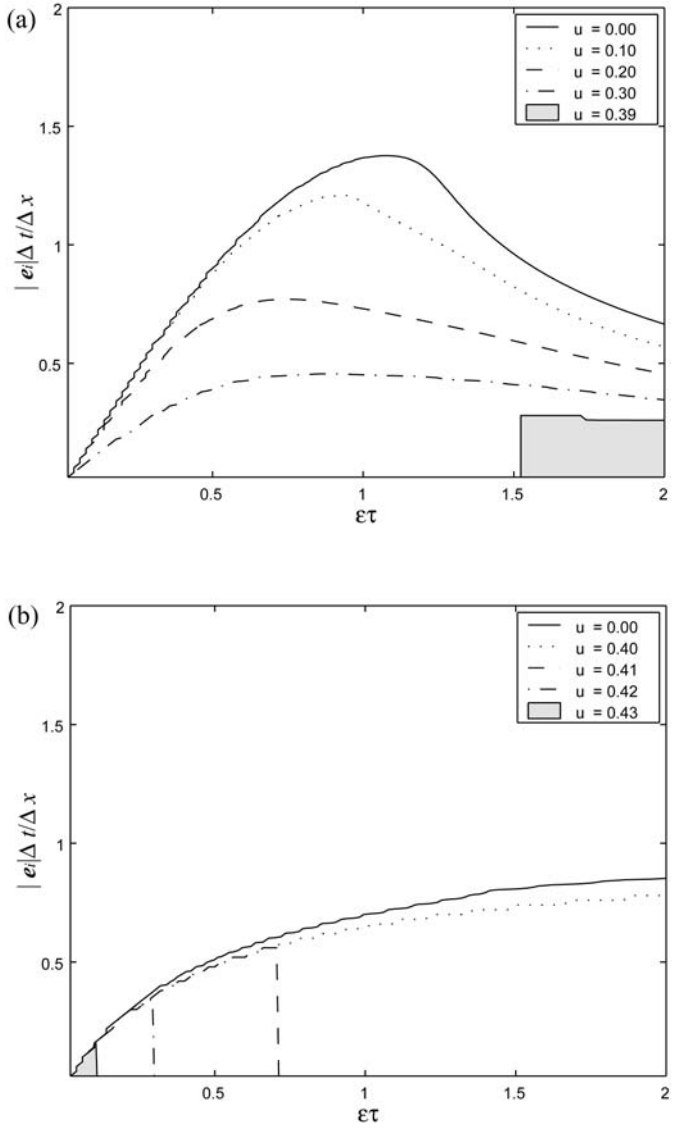

Fig. 3. Stability boundaries of the FDLBM applied the mean flow velocity to: (a) the explicit central difference; (b) the explicit upwind difference; (c) the semi-implicit upwind difference.

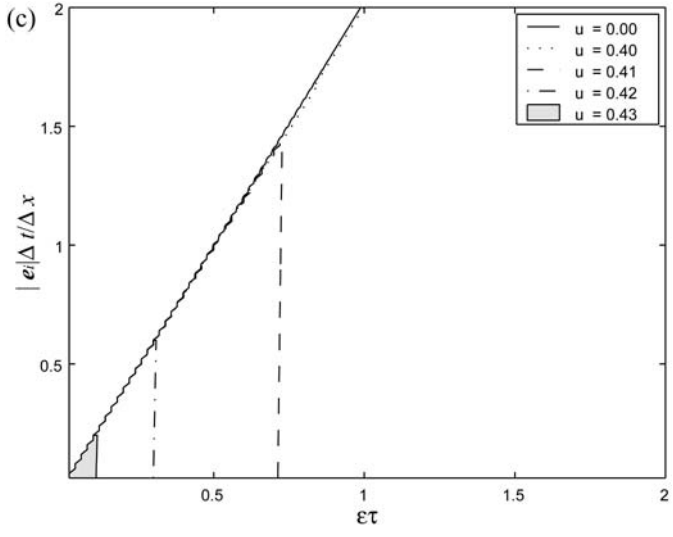

Fig. 3. (Continued).

Comparison of Eq. (1) and Eq. (25) reveals that the discretization generates the new term $(e_i)_\alpha \Delta x_\alpha(1-c_\alpha)/2$. This additional term is a coefficient on the second derivative of f_i with respect to $\mathbf{x}$, and is regarded as artificial viscosity or numerical diffusion.[21] Likewise, the artificial viscosities are given by $-(e_i)_\alpha^2 \Delta t/2$ and by $(e_i)_\alpha \Delta x_\alpha(1+c_\alpha)/2$ for the central difference and for the semi-implicit upwind difference schemes, respectively.

Schemes could be unstable by influence of negative artificial viscosity. The time step Δt should be small to lessen the effect of the negative artificial viscosity, $-(e_i)_\alpha^2 \Delta t/2$, on the central difference scheme. This requirement of time step for the central difference scheme is consistent with the necessity of small CFL number $|\mathbf{e}_i| \Delta t/\Delta x$ shown in Fig. 2a. Saying it differently, when using the central difference scheme, the FDLBM researchers cannot use large time step for stable numerical simulation.

For the explicit upwind difference scheme, when CFL number c_α is larger than unity, the artificial viscosity $(e_i)_\alpha \Delta x_\alpha(1-c_\alpha)/2$ is negative. To make the artificial viscosity positive and ensure numerical stability, it is necessary that the CFL number is smaller than unity. This requirement is compatible with the condition derived from von Neumann stability analysis, shown in Fig. 2b, that is, the maximum CFL numbers in stability regions are always smaller than unity. The standard definition of the Reynolds number Re for the hexagonal lattice is

$$\mathrm{Re} = \frac{LU}{\mu} = \frac{4LU}{\rho\varepsilon\tau} \tag{26}$$

where $L = N\,\Delta x$ is characteristic length, N is the number of lattice spaces, and U is characteristic flow velocity. Equation (26) indicates that the BGK relaxation time should be small or flow velocity should be large to obtain high Reynolds number. As is evident from Fig. 3b, the small CFL number is necessary for the explicit upwind difference scheme to stably simulate fluid dynamics with small BGK relaxation time and with large flow velocity. The small CFL number c_α brings about large artificial viscosity $(e_i)_\alpha\,\Delta x_\alpha(1-c_\alpha)/2$ as well, and ensures numerical stability. The explicit upwind difference scheme with appropriate CFL number is suitable for simulation of high Reynolds number flows.

For the semi-implicit upwind difference scheme, the artificial viscosity $(e_i)_\alpha\,\Delta x_\alpha(1+c_\alpha)/2$ is always positive. This large nonzero artificial viscosity degrades accuracy of the scheme, however, improves numerical stability. At the same CFL number, the artificial viscosity for semi-implicit upwind difference scheme is larger than that of the explicit upwind difference scheme.

6. CONCLUSION AND DISCUSSION

We analyzed the numerical stability of the FDLBM for the central difference scheme, for the explicit upwind difference scheme, and for the semi-implicit upwind difference scheme by means of von Neumann stability analysis. The stability boundary was shown as function of the CFL number, the BGK relaxation time, the mean flow velocity, and the wavenumber. The analysis indicated the following results: (1) The FDLBM eliminated the condition: $\tau > 0.5$, and is capable of simulating the high Reynolds number flow, when the CFL number is appropriately modulated, (2) as the BGK relaxation time is increased at constant CFL number, the central difference LB scheme could be numerically unstable, (3) the limits of maximum stable velocity are obtained around 0.39, 0.43, and 0.43 for the central difference, for the explicit upwind difference, and for the semi-implicit upwind difference schemes, respectively, (4) the upwind difference scheme is suitable for simulation of high Reynolds number flow, because it becomes more stable for high flow velocity, as the relaxation time is decreased.

Through the Taylor series expansion, the artificial viscosities are given by $-(e_i)_\alpha^2\,\Delta t/2$, $(e_i)_\alpha\,\Delta x_\alpha(1-c_\alpha)/2$, and $(e_i)_\alpha\,\Delta x_\alpha(1+c_\alpha)/2$ for the central difference, for explicit upwind difference, and for the semi-implicit upwind difference schemes, respectively. The investigation of artificial viscosities elucidated the following results: (1) The requirements for artificial viscosity is consistent with the conditions for numerical stability derived from von Neumann stability analysis, (2) the central difference scheme should adopt small time step for stable numerical simulation due to the negative artificial

viscosity, (3) for the explicit upwind difference scheme, to make the artificial viscosity positive, the CFL number should be smaller than unity, (4) to stably simulate high Reynolds number flows with explicit upwind difference scheme, the artificial viscosity becomes large, because the CFL number must be small, (5) for the semi-implicit upwind difference scheme, the large nonzero artificial viscosity degrades accuracy of the scheme, however, improves numerical stability.

These results substantiate that semi-implicit upwind difference scheme is the most numerically stable of all, and is capable of stably simulating flow dynamics with CFL number larger than unity. Actually we have confirmed that the semi-implicit upwind difference scheme could stably simulate the phase transition, although the CFL number is larger than unity.

We may, therefore, reasonably conclude that the upwind difference LB scheme is more stable than the conventional LBM, on the ground that it meets the high Reynolds number flow simulation and its limit of the maximum mean flow velocity is larger than that of the LBM. On the other hand, the conventional LBM includes the discretization error into viscous terms, resulting in second order accuracy both in space and time,[13] while the upwind difference LB scheme is first order accuracy. The shear viscosity for the LBM is given by $\mu = \rho(\tau - \frac{1}{2})/4$. The first and second parts in the viscosity are equivalent to the physical viscosity and to consequence of allowing for discretization error, respectively. Therefore, it is not necessary to consider artificial viscosity in the LBM. The LBM obtains the maximum value at small viscosity compared to the central difference LB scheme. The maximum stable flow velocity of the LBM equals to that of the central difference LB scheme (i.e., 0.39). The analysis also elucidated that the conventional LBM is an excellent scheme to get the second order accuracy.

REFERENCES

1. U. Frisch, B. Hasslacher, and Y. Pomeau, Lattice-gas automata for the Navier–Stokes equation, *Phys. Rev. Lett.* **56**:1505 (1986).
2. S. Chen and G. D. Doolen, Lattice Boltzmann method for fluid flows, *Ann. Rev. Fluid. Mech.* **30**:329 (1998).
3. G. R. McNamara and G. Zanetti, Use of the Boltzmann equation to simulate lattice-gas automata, *Phys. Rev. Lett.* **61**:2332 (1988).
4. J. D. Sterling and S. Chen, Stability analysis of lattice Boltzmann methods, *J. Comput. Phys.* **123**:196 (1996).
5. C. Bardos, F. Golse, and D. Levermore, Fluid dynamic limits of kinetic equations. I. Formal derivations, *J. Statist. Phys.* **63**:323 (1991).
6. J. E. Broadwell, Shock structure in a simple discrete velocity gas, *Phys. Fluds.* **7**:1243 (1964).

7. J. E. Broadwell, Study of rarefied shear flow by the discrete velocity method, *J. Fluid Mech.* **19**:401 (1964).
8. R. Gatignol, Kinetic theory for a discrete velocity gas and application to the shock structure, *Phys. Fluds.* **18**:153 (1975).
9. R. Gatignol, Kinetic theory boundary conditions for discrete velocity gases, *Phys. Fluds.* **20**:2022 (1977).
10. B. T. Nadiga and D. I. Pullin, A method for near-equilibrium discrete-velocity gas flows, *J. Comp. Phys.* **112**:162 (1994).
11. T. Inamuro and B. Sturtevant, Numerical study of discrete-velocity gases, *Phys. Fluds. A* **2**:2196 (1990).
12. J. Hardy, O. de Pazzis, and Y. Pomeau, Molecular dynamics of a classical lattice gas: Transport properties and time correlation functions, *Phys. Rev. A* **13**:1949 (1976).
13. N. Cao, S. Chen, S. Jin, and D. Martínez, Physical symmetry and lattice symmetry in the lattice Boltzmann method, *Phys. Rev. E* **55**:21 (1997).
14. H. Chen, S. Chen, W. H. Matthaeus, Recovery of the Navier–Stokes equations using a lattice-gas Boltzmann method, *Phys. Rev. A* **45**:R5339 (1992).
15. S. Chen, H. Chen, D. Martínez, and W. Matthaeus, Lattice Boltzmann model for simulation of magnetohydrodynamics, *Phys. Rev. Lett.* **67**:3776 (1991).
16. R. D. Richtmyer and K. Morton, *Difference Methods for Initial-Value Problems*, 2nd edn. (Interscience Pub., 1967), p. 70.
17. B. H. Elton, Comparisons of lattice Boltzmann and finite difference methods for a two-dimensional viscous Burgers equation, *SIAM J. Sci. Comput.* **17**:783 (1996).
18. X. He, Q. Zou, L.-S. Luo, and M. Dembo, Analytic solutions of simple flows and analysis of nonslip boundary conditions for the lattice Boltzmann BGK model, *J. Statist. Phys.* **87**:115 (1997).
19. D. R. Noble, S. Chen, J. G. Georgiadis, and R. O. Buckius, A consistent hydrodynamic boundary condition for the lattice Boltzmann method, *Phys. Fluids.* **7**:203 (1995).
20. Q. Zou and X. He, On pressure and velocity boundary conditions for the lattice Boltzmann BGK model, *Phys. Fluids.* **9**:1591 (1997).
21. P. J. Roache, *Computational Fluid Dynamics* (Hermosa Pub., 1976), p. 351.